

Synaptotagmin Has an Essential Function in Synaptic Vesicle Positioning for Synchronous Release in Addition to Its Role as a Calcium Sensor

Samuel M. Young, Jr.^{1,*} and Erwin Neher¹

¹Department of Membrane Biophysics, Max Planck Institute for Biophysical Chemistry, Am Fassberg 11, D-37077 Goettingen, Germany

*Correspondence: syoung@gwdg.de

DOI 10.1016/j.neuron.2009.07.028

SUMMARY

A multitude of synaptic proteins interact at the active zones of nerve terminals to achieve the high temporal precision of neurotransmitter release in synchrony with action potentials. Though synaptotagmin has been recognized as the Ca^{2+} sensor for synchronous release, it may have additional roles of action. We address this question at the calyx of Held, a giant presynaptic terminal, that allows biophysical dissection of multiple roles of molecules in synaptic transmission. Using high-level expression recombinant adenoviruses, in conjunction with a stereotactic surgery in postnatal day 1 rats, we overcame the previous inability to molecularly perturb the calyx by overexpression of a mutated synaptotagmin. We report that this mutation leaves intrinsic Ca^{2+} sensitivity of vesicles intact while it destabilizes the readily releasable pool of vesicles and loosens the tight coupling between Ca^{2+} influx and release, most likely by interfering with the correct positioning of vesicles with respect to Ca^{2+} channels.

INTRODUCTION

Two requirements have to be fulfilled so that synaptic vesicles (SVs) can be released synchronously within the short period of an action potential (AP): (1) they need a calcium sensor that can rapidly respond to an increase in calcium (Llinas et al., 1992) and (2) they have to be properly positioned near the Ca^{2+} channels, so that they can sense the nano/microdomain calcium signal (Adler et al., 1991). Synaptotagmins (syts) are a family of multifunctional double C2 membrane proteins (Chapman, 2008), a subset of which is associated with SVs (Takamori et al., 2006; Xu et al., 2007). In particular, *Syt1*, *Syt2*, and *Syt9* have been shown to be critical for synchronous release during action-potential-mediated release (Geppert et al., 1994; Littleton et al., 1993; Stevens and Sullivan, 2003; Xu et al., 2007). Recent studies demonstrated that syt's ability to bind calcium is necessary to mediate synchronous release in response to AP-driven Ca^{2+} influx (Fernandez-Chacon et al., 2002; Sun et al., 2007; Yoshihara and Littleton, 2002).

In addition to its calcium-sensing function, syt has been reported to interact with plasma membrane proteins (Bennett

et al., 1992; Hata et al., 1993; Leveque et al., 1992) and was hypothesized to link SVs to the calcium signal that drives synchronous release (Neher and Penner, 1994). Possible evidence for such a role came from morphological studies from syt knockout (KO) invertebrate synapses, which showed a decrease in the number of vesicles closely docked to the plasma membrane (Jorgensen et al., 1995; Reist et al., 1998). However, no tethering defects were detected in mammalian syt KO animals (Geppert et al., 1994). Subsequent work in squid used a peptide to interfere with the syt/neurexin interaction and completely blocked evoked release (Fukuda et al., 2000). This finding also suggested that syt plays a role in linking SV to sites of Ca^{2+} influx. However, this motif is also found in other molecules at the active zone (Krasnov and Enikolopov, 2000), so definitive conclusions could not be drawn.

Based on currently available data, definitive evidence for syt having a role in linking SV to the site of calcium influx is still lacking. Our aim is to determine if syt does indeed play a role in linking SV to the site of calcium influx. To demonstrate such a role, a dominant-negative mutant that would perturb release evoked by AP-like stimulation without interfering with the intrinsic Ca^{2+} sensitivity of the release apparatus is required. However, a mutant that might mediate such an effect must fulfill three requirements. (1) A perturbation should be placed at a site likely to mediate this role. (2) The mutation should not affect syt's ability to bind calcium. (3) It should not affect the proper folding of syt and its targeting to the synapse. In addition, the intrinsic calcium sensitivity of release must be measured at the synapse that overexpresses this dominant-negative mutant, so that any contributions of such effects to changes in AP-evoked release can be recognized.

A recent study on syt1 function identified a mutation in the C terminus of the C2B domain, R398,399Q, which did not affect calcium binding or the protein's folding (Arac et al., 2006; Xue et al., 2008) but was unable to rescue evoked release on a *Syt1* null background in autaptic neurons (Xue et al., 2008). Although this mutation is ideal to determine if syt plays role in addition to Ca^{2+} sensing, conclusions about how the mutation affects synaptic transmission were limited in this study using autaptic synapses because the intrinsic calcium sensitivity of release cannot be directly measured in this preparation. Specifically, defects in vesicle positioning or defects in the intrinsic calcium sensitivity cannot be dissected from one another. In fact, conclusions regarding the mechanism of the mutation have relied on conflicting results from liposomal assays, which were interpreted

either as an effect of syt on lipid mixing (Xue et al., 2008) or as a defect in syt's interaction with SNARE complexes (Gaffaney et al., 2008).

At the calyx of Held synapse, intrinsic Ca^{2+} sensitivity of the release apparatus can be determined by flash-photolysis of caged Ca^{2+} , and so defects in vesicle positioning can be discriminated against those affecting intrinsic calcium sensitivity. It has been demonstrated that SV positioning, also termed "positional priming," is important for synchronous release (Sakaba et al., 2005; Wadel et al., 2007). However, the calyx of Held preparation has severe restrictions regarding molecular perturbation studies: (1) there is no possibility of applying primary cell culture or organotypic slice culture techniques, and (2) typically paired recordings are done at postnatal day 8 (P8) and older, thus limiting the use of knockout mice, since the majority of genes knocked out for synaptic transmission result in embryonic lethality. This has limited the preparation's use so far in generating a more complete understanding of presynaptic function at the molecular level.

Since the calyx would be the ideal synapse to address a variety of questions regarding the functional roles of synaptic proteins, we made a major effort to develop molecular tools for this preparation. New recombinant Adenoviral (rAd) vectors with high levels of transgene expression and a novel rat stereotactic surgery at P1 had to be established. Since the calyx of Held expresses syt2 (Pang et al., 2006a), a reciprocal mutation of rat syt1 R398,399Q was cloned into rat syt2 (syt2). The mutant syt2 R399,400Q was overexpressed at the rat calyx of Held using these rAd vectors in conjunction with P1 stereotactic surgery, and its effects on synaptic transmission were analyzed. Here we show that synchronous release, triggered by an AP, is sharply reduced, while the intrinsic Ca^{2+} sensitivity of vesicles is unchanged. In addition, the releasable vesicle pool is reduced when overexpression of the mutant protein is strong. We conclude that syt has an essential role in positioning vesicles at the active zone in addition to being the calcium sensor for synchronous release.

RESULTS

Development of Novel Surgery and a Recombinant Adenoviral Expression System to Analyze the Roles of Synaptotagmin at the Rat Calyx of Held

Despite its strengths for biophysical studies, the calyx of Held synapse has significant weaknesses as a target for the application of modern molecular biology techniques to perturb the synapse. This has limited its suitability so far for generating a more complete understanding of molecular mechanisms underlying presynaptic function. Recent attempts to establish these techniques at the calyx synapse have had limited success. Particularly, it had been impossible to perturb the synapse's function (Wimmer et al., 2004). Thus, a new platform technology to molecularly perturb the calyx had to be developed. In order to do so and to analyze syt's various roles in synaptic transmission, two strategies were employed in parallel: (1) creation of a high-level expression viral vector and (2) development of a novel stereotactic surgery on P1 rat pups to deliver these new viral vectors.

In order to achieve high levels of expression, a cassette for *in vivo* expression, called pUNISHER, was created. Figure 1A shows the final structure of the neurospecific pUNISHER expres-

sion cassette. The rAd vector coexpressed syt2 R399,400Q or syt2 (Figure 1B) from the pUNISHER cassette and EGFP from the synapsin promoter independently of each other (Figure 1C). This allows for identification of all infected calyces by EGFP. To check for full-length syt2 R399,400Q protein expression, primary hippocampal neurons were infected with the R399,400Q virus and subjected to western blot analysis. Figure 1D shows that full-length syt2 R399,400Q protein was expressed.

Additionally, a novel stereotactic surgery on P1 rat pups was developed to deliver the rAd vectors at the calyx of Held. To ensure that the effects of the mutation were not due to nonspecific effects of overexpression, P1 rat pups were also with injected with rAd that overexpressed syt2 from the pUNISHER cassette. Figure 1E shows EGFP-positive calyces, demonstrating successful targeting of the cochlear nucleus, where the globular bushy cells are located that give rise to the calyx of Held synapse.

Overexpression of syt2 R399,400Q Results in a Dominant-Negative Phenotype in Response to AP-like Stimulation

In order to determine the syt2 R399,400Q effects on synchronous release, calyces expressing the mutant syt2 or syt2 were identified as being EGFP positive and were subsequently used for simultaneous presynaptic and postsynaptic patch-clamp recording in the whole cell configuration. Presynaptic and postsynaptic compartments were voltage clamped to -80 mV, short AP-like depolarizations were applied to the calyx, and the AMPAR-mediated postsynaptic currents were measured. The effects of the syt2 R399,400Q mutation on AP-like release were then quantified (Figures 2A1, 2A2, 2A3, and 2A4). Presynaptic overexpression of this protein resulted in a severe reduction or a complete loss of the EPSC, though varying levels of penetrance of the syt2 R399,400Q phenotype were found (Table 1, Figure 2B). The 4-fold reduction of the mean EPSC was not due to a change in the presynaptic Ca^{2+} current (Table 1, Figure 2C). In addition, syt2 overexpression resulted in a 1.8-fold increase of the mean EPSC that was not due to a change in the presynaptic Ca^{2+} current (Table 1, Figure 2C), though the post hoc test was not sensitive enough to prove a highly significant difference. These values of the presynaptic Ca^{2+} current are similar to previous reports at the calyx of Held (Sakaba, 2006; Sakaba and Neher, 2001a). In addition to the reduction in synchronous release, the syt2 R399,400Q mutation also increased the synaptic delay time for evoked release compared to control or syt2 (Table 1, Figure 2D). These results show that syt2 R399,400Q results in a dominant-negative phenotype, which is similar to the phenotype of the R398,399Q syt1 mutation on the syt null background in hippocampal autapses (Xue et al., 2008), and not due to nonspecific effects of overexpression of syt2. This result confirms that this region of syt is critical to trigger synchronous release.

Overexpression of syt2 R399,400Q Results in an Increase in Paired Pulse Facilitation and Facilitation in Response to 100 Hz Stimulation

Since changes in the paired pulse ratio (PPR) are indirect measures of initial release probabilities, Xue et al. (2008) measured

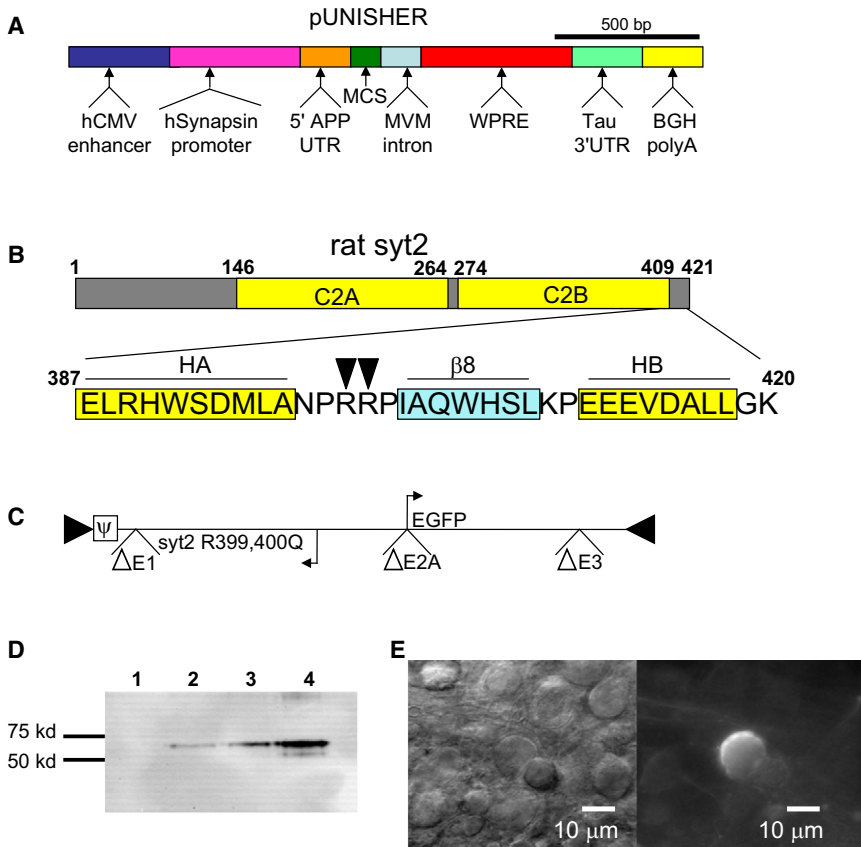


Figure 1. Expression of syt2 R399,400Q in the Rat Calyx of Held

(A) Schematic of the pUNISHER expression cassette. pUNISHER is 2.184 kb long. Optimized transcriptional, posttranscriptional, and translational signals are shown: the human CMV enhancer (hCMV), human synapsin promoter, 5' amyloid precursor protein (APP), untranslated region (UTR), multiple cloning site (MCS), minute virus of mice (MVM) intron, woodchuck post-transcriptional regulatory element (WPRE), tau 3'UTR, and bovine growth hormone (BGH) polyadenylation signal (poly A).

(B) Schematic illustration of syt2 with location of mutated residues in the C terminus of the C2B domain. Location of HA and HB helices in the C2B domain are highlighted yellow; location of the $\beta 8$ strand is highlighted in light blue. Black triangles indicate the position of R399,400.

(C) Schematic of the rAd syt2 R399,400Q virus. The black triangles represent the viral inverted terminal repeats. The packaging signal Ψ is highlighted by the open box.

(D) Expression of syt2 R399,400Q protein from the pUNISHER rAd vectors. Primary hippocampal neurons were infected with 1×10^4 , 1×10^5 , or 1×10^6 particles of syt2 R399,400Q rAd virus. Lane 1: uninfected neurons. Lane 2: 1×10^4 particles. Lane 3: 1×10^5 particles. Lane 4: 1×10^6 particles.

(E) EGFP-positive calyces from P8 Wistar rats injected with syt2 R399,400Q virus at P1 and sacrificed 7 days later. Transverse brainstem slices containing the MNTB were made. Left panel shows the transillumination image and the right panel is the corresponding fluorescence image. Images were made using a 60x objective (Olympus).

PPRs in hippocampal autapses. They found an increase in the PPR and frequency-dependent facilitation with syt1 R398,399Q and concluded that this mutation lowers initial release probability. It is known that calcium current facilitation can play a role in facilitation of the EPSC at 100 Hz stimulation (Borst and Sakmann, 1998; Cuttle et al., 1998; Xu and Wu, 2005). In order to test facilitation of the EPSC independent of calcium current facilitation, we applied a paired pulse stimulation protocol (50 Hz stimulation) that was designed to result in similar calcium charge integrals between the first and second stimulation pulse. Figure 3 shows that on average syt2 R399,400Q calyces exhibited paired pulse facilitation (PPF), while control calyces and syt2-overexpressing calyces typically exhibited slight paired pulse depression (PPD) (Table 1). Increases in the PPR were seen in the absence of calcium current facilitation or inactivation (Table 1, Figure 3C). Based on these results, we conclude that the R399,400Q mutation reduces initial release probability and results in an increase in PPF, although we cannot exclude the involvement of mechanisms other than a reduction of the initial release probability.

In acute slices, the calyx of Held synapse depresses when stimulated with a 100 Hz pulse train in extracellular solution containing 2 mM Ca^{2+} and 1 mM Mg^{2+} (Schneppenburger et al.,

1999). Thus, to further demonstrate that syt2 R399,400Q lowers the initial release probability, the calyces were stimulated with 20 AP at 100 Hz. Figures 4A1 and 4A2 show that in control calyces or calyces overexpressing syt2, the terminal undergoes frequency-dependent depression, while Figure 4A3 shows that syt2 R399,400Q calyces undergo pronounced frequency-dependent facilitation. On average control synapses or syt2 synapses quickly depress, while (on average) R399,400Q synapses strongly facilitate and stay facilitated throughout the train (Figure 4C). Based on the results of Figures 3 and 4, it can be concluded that overexpression of syt2 R399,400Q results in a lowering of the initial release probability.

Overexpression of syt2 R399,400Q Results in a Reduction of the Total Readily Releasable Pool and Slows the Kinetics of the Fast Component of Release with No Change in mEPSC Frequency

Using sucrose to study the RRP of autaptic hippocampal neurons, it was concluded that the readily releasable pool (RRP) size was unchanged by expression of the syt1 R398,399Q mutation (Xue et al., 2008). However, it is unclear what the exact mechanism of sucrose-induced release is and how it relates to physiological measurements of synaptic release (Moulder and

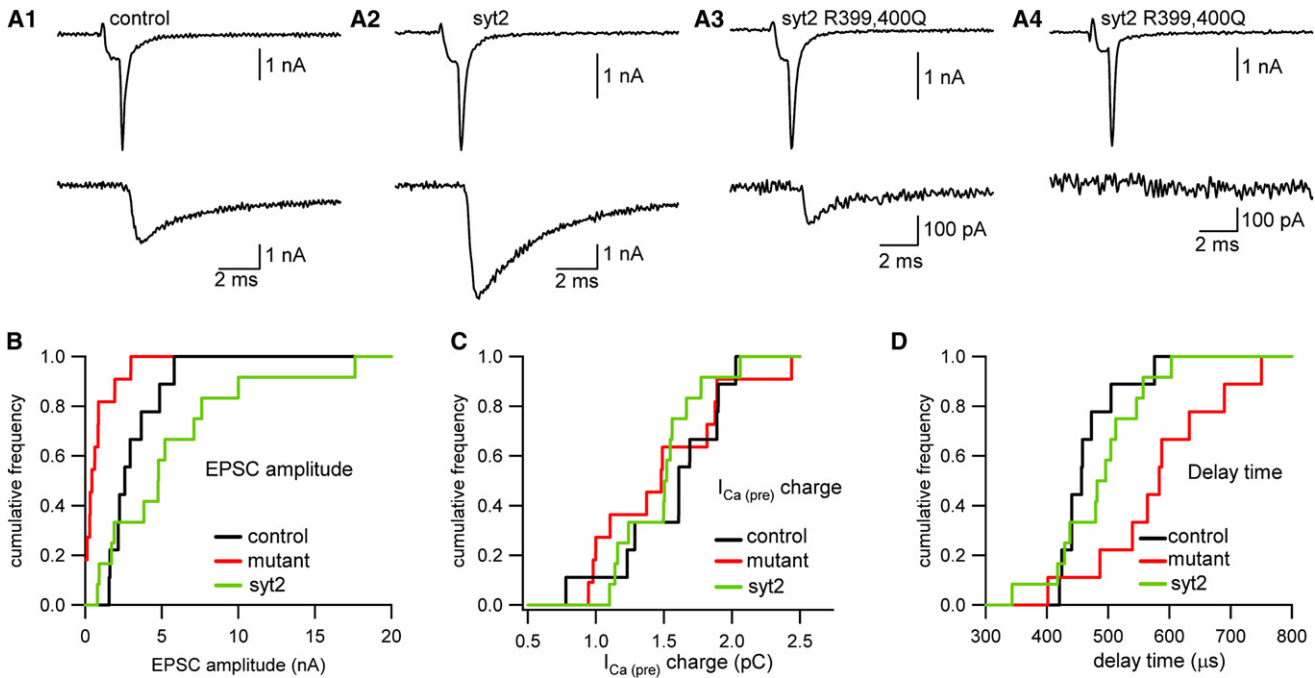


Figure 2. Overexpression of syt2 R399,400Q Results in a Reduction of the EPSC with No Change in the Presynaptic Calcium Current, but an Increase in the Synaptic Delay

(A) Representative traces of EPSC (lower) and presynaptic calcium current (upper) recordings from P8 to P9 rats injected with rAd syt2 R399,400Q virus, rats injected with rAd syt2 virus, or age-matched control animals not injected with virus. EPSCs and presynaptic calcium currents are compared between control calyces (A1) and calyces expressing syt2 (A2), syt2 R399,400Q at medium penetrance (A3), or syt2 R399,400Q at strong penetrance (A4). Presynaptic and post-synaptic compartments were voltage clamped to -80 mV and stimulated with an AP-like short depolarization (1 ms square wave pulse from -80 mV to $+40$ mV). (B) Cumulative frequency histograms of EPSC amplitudes from syt2 (green traces), syt2 R399,400Q (red traces), and control animals (black traces). ($n = 9$ control, $n = 12$ syt2, $n = 11$ syt2 R399,400Q).

(C) Same analysis and display as in (B), but using presynaptic calcium current charge integrals.

(D) Same analysis and display as in (B), but using synaptic delay time. Delay was measured as described in the [Experimental Procedures](#).

Mennerick, 2005). Since the calyx of Held presynapse can be voltage clamped, one can measure the size of the physiologically relevant RRP using a long-lasting depolarization, which depletes the pool completely. Deconvolving the resulting EPSCs and integrating the release rates, one obtains a measure for pool size (Neher and Sakaba, 2001a; Sakaba and Neher, 2001a).

To analyze how the syt2 R399,400Q mutation affected the RRP, terminals were stimulated with a 50 ms depolarizing pulse and EPSC amplitudes and synaptic delays were determined. Representative traces show clear effects of the syt2 R399,400Q overexpression on the peak EPSC amplitude and the kinetics of the responses as compared to those of control (Figures 5A1, 5A2, and 5A3). The overexpression of R399,400Q syt2 resulted in a severe reduction of EPSCs, as compared to control, and syt2 overexpression (Table 1), though varying levels of penetrance of the syt2 R399,400Q phenotype were found (Figure 4B). The reduction of the EPSCs was not due to a loss of presynaptic Ca^{2+} currents as there was no difference in presynaptic Ca^{2+} currents between R399,400Q, control, and syt2 calyces (Figure 5C, Table 1). Similar to the case of synaptic delay in response to AP-like stimulation, the syt2 R399,400Q mutation also increased the synaptic delay time for the long depolarization (Table 1).

To accurately measure the RRP at the calyx, a deconvolution routine was employed that accounts for spillover current contributions (Neher and Sakaba, 2001a, 2001b; Sakaba and Neher, 2001b). Also, it has been shown that the RRP can be separated into two components when 0.5 mM EGTA is included in the presynaptic patch pipette solution. These are interpreted to represent a “fast pool” and a “slow pool” of vesicles, which on average contribute equally to the total RRP (Sakaba and Neher, 2001a). The fast pool was shown to be composed of those vesicles that are mainly responsible for synchronous release (Sakaba, 2006). To measure the RRP, traces from Figure 6 were deconvolved and integrated. Figure 6A shows an example of the deconvolution of postsynaptic traces. Figure 6B shows that the overexpression of the syt2 R399,400Q mutation drastically alters peak vesicle release rates compared to those of control and syt2, and confirms the reduction in the peak EPSC amplitude shown in Figure 5B. It should be noted that one cell pair from Figure 5 was not included in the deconvolution analysis, because its EPSCs were too small to determine adequate deconvolution parameters. To test how the kinetics of release were affected, the traces of Figure 6B were normalized with respect to their peak release rates (Figure 6C). This revealed a significant increase in the relative amount of asynchronous

Table 1. Summary of Synaptic Responses from Control, *syt2*-Overexpressing, and *syt2* R399,400Q-Overexpressing Calyx of Held Synapses

Parameter	Control (n)	<i>syt2</i> (n)	<i>syt2</i> R399,400Q (n)	Statistic Test	Post Hoc Test
1 ms AP-like ESPC (nA)	3.04 ± 0.489 (9)	5.51 ± 1.37 (12)	0.758 ± 0.276 (11)	Kruskal-Wallis, p < 0.001	Dunn's test control versus mutant p < 0.05, mutant versus <i>syt2</i> p < 0.001, control versus <i>syt2</i> n.s.
1 ms AP-like Ca ²⁺ charge integral (pC)	1.59 ± 0.132 (9)	1.48 ± 0.0821 (12)	1.49 ± 0.144 (11)	one-way ANOVA, n.s.	
1 ms AP-like EPSC synaptic delay (μs)	466 ± 16.2 (9)	581 ± 31.1 (12)	483 ± 20.3 (9)	one-way ANOVA, p < 0.01	Tukey test control versus mutant p < 0.01, mutant versus <i>syt2</i> p < 0.05, control versus <i>syt2</i> n.s.
EPSC paired pulse ratio	0.972 ± 0.0481 (9)	0.904 ± 0.0622 (11)	1.35 ± 0.101 (7)	one-way ANOVA, p < 0.001	Tukey test control versus mutant p < 0.01, mutant versus <i>syt2</i> p < 0.001, control versus <i>syt2</i> n.s.
Ca ²⁺ charge integral paired pulse ratio	1.01 ± 0.00620 (9)	1.00 ± 0.00313 (11)	1.00 ± 0.00904 (7)	one-way ANOVA, n.s.	
Long depolarization EPSC (nA)	20.8 ± 3.49 (8)	24.8 ± 3.51 (9)	8.28 ± 2.68 (8)	one-way ANOVA, p < 0.01	Tukey test control versus mutant p < 0.05, mutant versus <i>syt2</i> p < 0.01, control versus <i>syt2</i> n.s.
Long depolarization Ca ²⁺ charge integral (pC)	69.2 ± 2.92 (8)	69.2 ± 3.94 (9)	71.7 ± 4.93 (8)	one-way ANOVA, n.s.	
Long depolarization synaptic delay (ms)	1.86 ± 0.0996 (8)	1.71 ± 0.0928 (9)	3.10 ± 0.515 (8)	Kruskal-Wallis, p < 0.001	Dunn's test control versus mutant p < 0.05, mutant versus <i>syt2</i> p < 0.001, control versus <i>syt2</i> n.s.
RRP size (vesicles)	3454 ± 398.2 (8)	4125 ± 551.3 (9)	2090 ± 619.8 (7)	one-way ANOVA, p < 0.05	Tukey test control versus mutant n.s., mutant versus <i>syt2</i> p < 0.05, control versus <i>syt2</i> n.s.
Peak vesicle release rates (vesicles/ms)	1034 ± 222.7 (8)	1307 ± 231.9 (9)	344 ± 116 (7)	one-way ANOVA, p < 0.02	Tukey test control versus mutant n.s., mutant versus <i>syt2</i> p < 0.05, control versus <i>syt2</i> n.s.
mEPSC frequency (Hz)	0.762 ± 0.184 (6)	0.562 ± 0.103 (8)	0.582 ± 0.126 (8)	one-way ANOVA, n.s.	
mEPSC amplitude (pA)	35.3 ± 2.13 (6)	39.5 ± 1.97 (8)	37.7 ± 2.82 (8)	one-way ANOVA, n.s.	
K ₁₀ (μM) ^a	15.8 ± 2.15		19.2 ± 2.36	random permutation test, p = 0.263868, n.s.	

Values are given mean ± SEM. Statistical significance was considered for p < 0.05.

^aMean ± bootstrap estimate of the SEM.

release in those mutant calyces that showed small EPSCs. Integration of release rates for the duration of the depolarizing pulse showed that the mutation causes a reduction in the RRP as compared to that of control (Table 1). However, there was large variability in the *syt2* R399,400Q RRP pool size (Figure 6D), probably due to varying penetrance of the mutant phenotype. To determine the effects of the mutation on the kinetics of the fast component, integrated traces were normalized to their respective total number of vesicles released during the depolarizing pulse. Figure 6E shows that some traces from the mutant phenotype had a significantly slowed down fast component, while others were comparable to those of control.

Since other mutations in *syt* have caused an increase in miniature EPSC (mEPSC) frequency, it was possible that the reduc-

tion in the RRP might have been due to such an effect. To test this hypothesis we measured the frequency of mEPSCs at calyces overexpressing either *syt2* or *syt2* R399,400Q, or at the calyces of noninjected animals. Since we had known that EGFP expression levels correlated with the penetrance of the mutant phenotype (Figure S1 available online), we only recorded from principal cells of medial nucleus of the trapezoid body (MNTB) that were contacted by calyces that had high levels of EGFP expression. Figure 7A shows example traces from the mEPSC recordings, while Figure 7B demonstrates that there was no change in the average miniwaveform between *syt2*, *syt2* R399,400Q, and control. Average mEPSC frequency was unchanged between *syt2* and *syt2* R399,400Q compared to that of control (Table 1, Figure 7C). Additionally, the amplitude

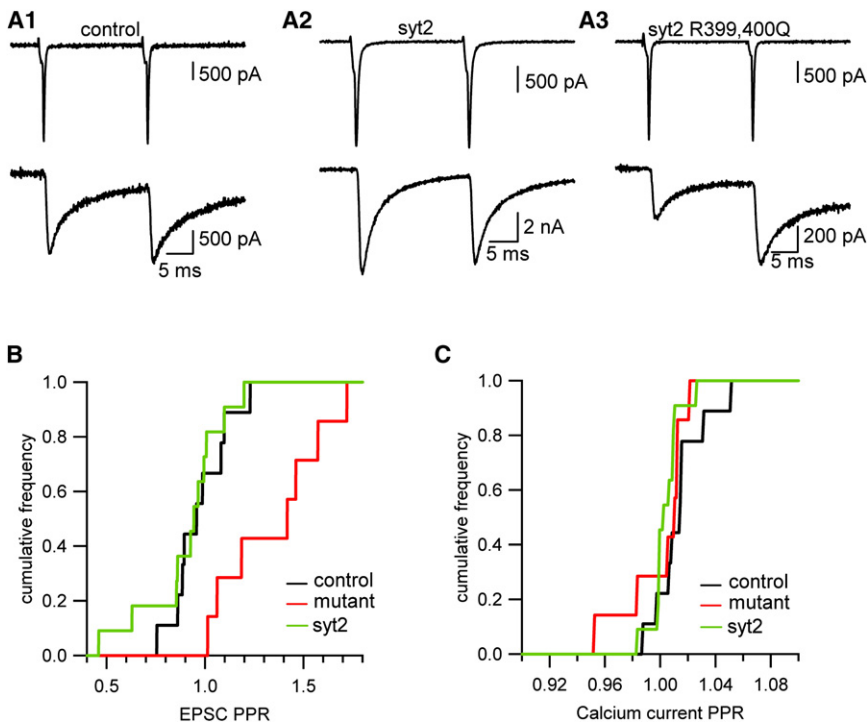


Figure 3. Overexpression of syt2 R399,400Q Results in an Increase in the EPSC PPR with No Change in the Presynaptic Calcium Current PPR

(A) Representative traces of EPSC (lower) and presynaptic calcium current (upper) recordings from P8 to P9 rats injected with rAd syt2 R399,400Q virus, rats injected with rAd syt2 virus, or age-matched control animals not injected with virus. Control calyces (A1), syt2 calyces (A2), or syt2 R399,400Q calyces (A3) were identified and the presynaptic and postsynaptic compartments were voltage clamped to -80 mV. Calyces were stimulated with two 1 ms depolarizing square wave pulses from -80 mV to $+40$ mV at a 20 ms interstimulus interval.

(B) Cumulative frequency histograms of PPR values from syt2, syt2 R399,400Q, and control animals. Control (black traces), syt2 (green traces), and syt2 R399,400Q (red traces) are shown. ($n = 9$ control, $n = 11$ syt2, $n = 7$ syt2 R399,400Q).

(C) Same as in (B), except that presynaptic calcium current PPR charge integrals of syt2, syt2 R399,400Q, and control animals are shown.

between syt2, syt2 R399,400Q, or control animals (Table 1, Figure 7D) was unchanged.

Based on the results in Figures 5, 6, and 7, it can be concluded that overexpression of syt2 R399,400Q results in a reduction of the RRP with no change in driving Ca^{2+} current or change in mEPSC frequency. Synaptic delays were increased and a corresponding slowdown in the fast component of release of the RRP was observed. The reduction in the RRP size is contrary to what has been reported regarding the sucrose-sensitive pool in hippocampal autapses of this mutation (Xue et al., 2008).

Overexpression of syt2 R399,400Q Does Not Change the Intrinsic Ca^{2+} Sensitivity of the Release-Ready Vesicles

Though the syt2 R399,400Q mutation revealed massive changes in release kinetics upon stimulation by depolarization, these experiments do not specify how the mutation is interfering with release. Based on the depolarization data and the finding that the Ca^{2+} currents are unchanged, there are two possible mechanisms: (1) a change in the (presynaptic release machinery's) intrinsic Ca^{2+} sensitivity of release or (2) a defect in the efficiency of coupling between Ca^{2+} influx and vesicle release. The latter mechanism might reflect a role of syt2 in the proper positioning of vesicles close to the sites of Ca^{2+} influx.

Because the calyx of Held synapse is amenable to flash-photolysis of caged Ca^{2+} and ratiometric Ca^{2+} imaging, it allows one to elevate Ca^{2+} uniformly in the terminal and to measure the intrinsic calcium sensitivity of release (Bollmann et al., 2000; Schneggenburger and Neher, 2000). Therefore we can ask whether the mutant phenotype results from a change in the proper positioning of vesicles relative to Ca^{2+} channels or a change in the intrinsic Ca^{2+} sensitivity of release. To test for the latter, flash-photolysis of caged Ca^{2+} was carried out on

calyces expressing syt2 R399,400Q. Since overexpression of syt2 R399,400Q led to varying penetrance of the mutant phenotype, it was important to compare only those terminals that exhibited a strong mutant phenotype when compared to wild-type terminals. Criteria for inclusion of mutant cell pairs in the data set were based on their responses to depolarization (See Experimental Procedures).

In order to measure the remaining RRP, a long depolarizing pulse (50 ms) was given 50 ms after flash-photolysis of DM-nitrophen. Figure 8A shows example traces from a control (Figure 8A1) and a syt2 R399,400Q-expressing terminal (Figure 8A2) in which intracellular calcium, $[\text{Ca}^{2+}]_i$, was elevated to levels above $10 \mu\text{M}$. In both cases, flashing to the same $[\text{Ca}^{2+}]_i$ ($\sim 18 \mu\text{M}$ control, $\sim 17 \mu\text{M}$ mutant) completely depleted all releasable vesicles, since subsequent depolarizing stimulation did not result in any further release in both cases. Sizes of these pools were determined to be identical to the values measured by stand-alone 50 ms long depolarizations (control, 0.963 ± 0.0230 , $n = 8$; mutant, 0.996 ± 0.0235 , $n = 9$).

To compare the intrinsic Ca^{2+} sensitivity of release between the mutant and control calyces, peak release rates from the deconvolution analysis were divided by each cell pair's respective RRP to give the peak release rate per vesicle. Data were obtained for eight control cell pairs and nine cell pairs expressing syt2 R399,400Q that fulfilled the criteria described above. Peak release rates per vesicle were then plotted on a log-log plot as a function of post-flash $[\text{Ca}^{2+}]_i$ (Figure 8B). The plotted data was then fitted with the five-site kinetic release model described by Schneggenburger and Neher (2000) using the fitting routine of Wang et al. (2008). Using analysis of the residuals (see Experimental Procedures) (control, -0.008235 ± 0.05914 , $n = 17$; mutant, -0.0762 ± 0.07545 , $n = 15$), we were able to reject the

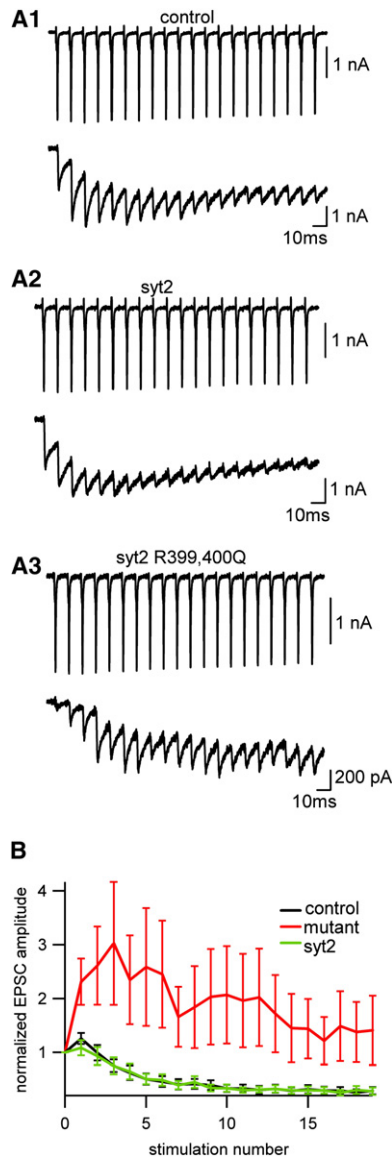


Figure 4. Overexpression of syt2 R399,400Q Results in an Increase in Facilitation in Response to 100 Hz Stimulation

(A) Representative traces of EPSC (bottom traces) and presynaptic calcium current recordings (top traces) from P8 to P9 rats that had been injected with rAd syt2 virus (A2) or rAd syt2 R399,400Q virus (A3), or age-matched control animals (A1). Calyces were stimulated with twenty 1 ms depolarizing square wave pulses from -80 mV to $+40$ mV at 100 Hz.

(B) Relative EPSC peak amplitudes were measured and then normalized to each individual trace's first EPSC peak amplitude (see *Experimental Procedures*) ($n = 5$ syt2 R399,400Q, $n = 5$ control, $n = 8$ syt2). Data presented as mean \pm SEM.

hypothesis that the two groups were different (t test, two-tailed, $p > 0.47$). More specifically we could also reject the hypothesis that the mutant flash rates were more than 1.63-fold slower than the control flash rates (one-sample t test, one-tailed, $p < 0.05$; *Figure 7B*). The parameters from the model fits were also used to determine the K_{10} , the Ca^{2+} concentration at which the

peak release rate is 10% of the maximal rate (Neher and Sakaba, 2008). The K_{10} of the mutant terminals, $19.2 \pm 2.36 \mu\text{M}$, and that of the control, $15.8 \pm 2.15 \mu\text{M}$, indicate little difference in the intrinsic calcium sensitivity of release between the mutant and control terminals (*Table 1*).

Comparable peak release rates led to the expectation that the synaptic delays of the EPSCs from the flash experiments should also be similar between mutant and control. Synaptic delays in response to flash-photolysis of caged Ca^{2+} were therefore determined for the control and syt2 R399,400Q calyces at the different $[Ca^{2+}]_i$ (see *Experimental Procedures*). We found that the delays of mutants were very close to those of control (grand mean ratio, 1.123 ± 0.1246). This supports the model fits (of the data) and indicates that the mutation does not cause any significant change in the intrinsic calcium sensitivity of release.

These results in combination with a loss of the fast component of release, as revealed by deconvolution, strongly suggest that this region of syt2, and syt in general, plays an important role in positional priming of vesicles at the active zone, in addition to being the calcium sensor for synchronous release. The decrease in pool size points to further roles of syt2 that are addressed in the *Discussion*.

DISCUSSION

Positional priming, which has been proposed as a process of alignment of vesicles at sites where Ca^{2+} channels cluster in the active zone, is essential for synchronous release (Wadel et al., 2007). However, the molecules involved in its regulation have remained elusive. Here, it is shown that overexpression of the R399,400Q mutation in syt2 at the calyx of Held causes an increase in the synaptic delay and a slowing of the kinetics of synchronous release elicited by depolarization (*Figures 2, 5, and 6*), while the intrinsic Ca^{2+} sensitivity of exocytosis, as measured by flash-photolysis of caged Ca^{2+} , is not changed (*Figure 8*). These results, together with the finding that Ca^{2+} currents are not affected by the mutation, leaves the conclusion that syt is involved in positional priming of vesicles at the active zone as the only reasonable explanation. In addition we found that the perturbation leads to a decrease in the releasable vesicle pool.

Development of the Technology for Molecular Studies at the Calyx of Held

For the uncovering of roles of syt in addition to its well-studied Ca^{2+} sensor function, new high-level in vivo expression viral vectors had to be generated and a novel P1 stereotactic rat surgery (*Figure 1*) had to be developed. The use of the pUNISHER cassette to express syt2 R399,400Q in second-generation rAd vectors resulted in a dominant-negative phenotype at the calyx of Held synapse similar to the phenotype reported for the syt1 R398,399Q mutant on the *Syt1* null background in hippocampal autapses (Xue et al., 2008). The similarity of phenotypes rules out that the effects seen in our studies are due to either toxicity of the second-generation rAd vectors or the overexpression of syt2. The second-generation rAd vectors used here are deleted for E2a, which removes any potential side effects described for

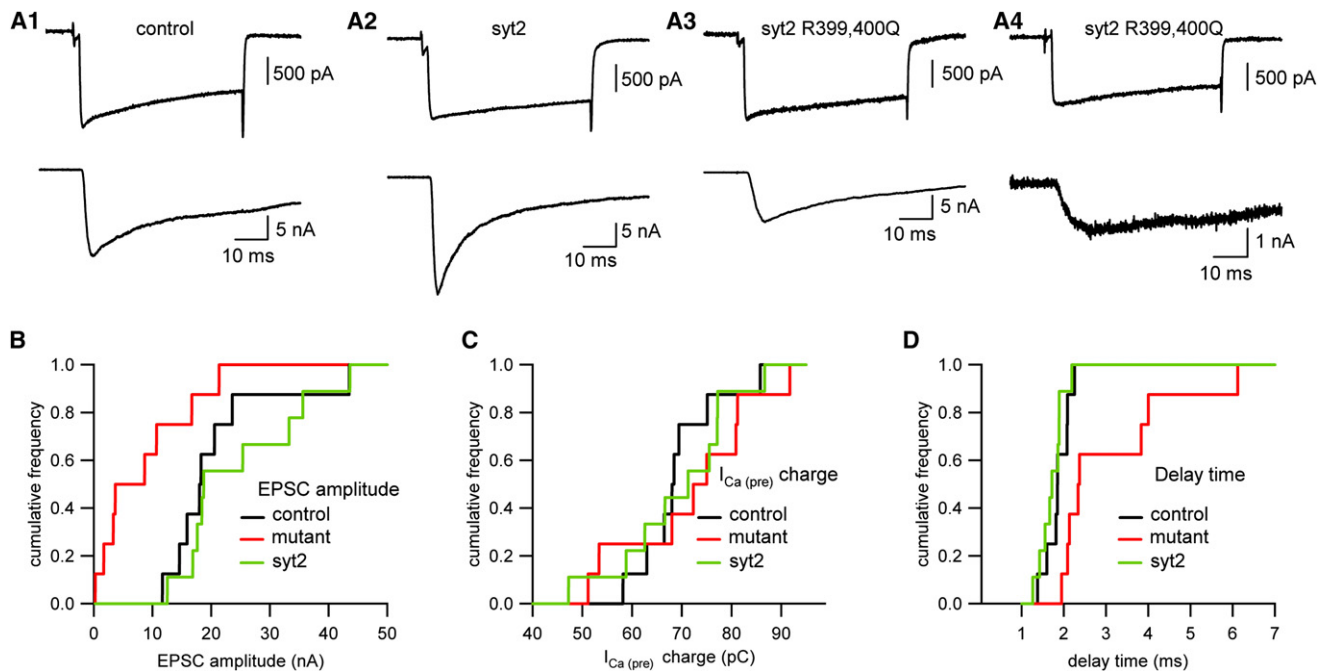


Figure 5. Responses to Long-Lasting Depolarizations Are Smaller and Delayed after Overexpression of syt2 R399,400Q

(A) The figure is laid out identically to Figure 2 (A1, control; A2, syt2; A3, weak penetrance; A4, high penetrance). In these traces, calyces were stimulated with a 2 ms -80 mV to $+70$ mV pulse followed by a 50 ms square wave pulse to 0 mV.

(B) Cumulative frequency histograms of EPSC amplitudes from syt2 (green traces), syt2 R399,400Q (red traces), and control animals (black traces). ($n = 8$ control, $n = 9$ syt2, $n = 8$ syt2 R399,400Q).

(C) Same as in (B), except that presynaptic calcium current charge integrals are displayed.

(D) Same analysis and display as in (B), but showing synaptic delay times.

the first-generation rAd vectors (Zhou and Beaudet, 2000). Finally, overexpression of syt2 itself at the calyx did not cause a reduction in either the EPSC or presynaptic calcium current (Figures 2, 3, 4, 5, and 6).

However, overexpression of syt2 R399,400Q displayed some variability in the penetrance of the mutant phenotype (Figures 2, 3, 4, 5, and 6). This variability was likely due to variability of syt2 R399,400Q protein levels relative to native syt2 levels in calyces. Variations in expression were suggested by variable EGFP intensities of transduced calyces, and we found a correlation between EGFP intensity and mutant phenotype. Cell pairs, which had a higher EGFP intensity-to-background ratio, resulted in stronger mutant phenotypes (Figure S1). Since calyces have a large variability in vesicle numbers (Schneppenburger and Forsythe, 2006), different levels of syt2 R399,400Q between calyces may be required to achieve negative dominance.

Though syt2 R399,400Q acts a dominant-negative, we could not distinguish how it achieves negative dominance. pUNISHER is an extremely high-level expression cassette and, in combination with multiple copies of rAd particles per neuron, will result in high levels of mutant syt2 relative to native syt2. This will be similar to expression of syt from other viral expression systems relative to native syt (Han et al., 2004; Stevens and Sullivan, 2003). The increased amount of the mutant syt2 relative to native syt2 will result in a higher probability that mutant syt2 is incorporated into SVs on the basis of the law of mass action. Thus, the

mutant syt dominant negative is likely to act by preventing native syt2's participation in exocytosis.

Syt2 R399,400Q Results in a Vesicle Positioning Defect

Though syt's role as a calcium sensor for synchronous release is well established (Sun et al., 2007), other roles of this molecule in synaptic transmission have been discussed (Verhage and Sorensen, 2008). Given the complexity of neurotransmitter release, it is not surprising that synaptic proteins are multifunctional. Earlier work has shown that interference with synprint sites on calcium channels may affect vesicle positioning, which results in a loss of the synchronous component (Mochida et al., 1996). In addition, previous studies have assigned a role in positional priming to VAMP/synaptobrevin (Sakaba et al., 2005; Wadel et al., 2007). In these studies, calyces were infused with tetanus toxin (Sakaba et al., 2005), a peptide mimicking the N terminus of VAMP/synaptobrevin, or an antibody raised against the N terminus (Wadel et al., 2007). The analysis of the depolarization responses using deconvolution showed a change in the release kinetics of the fast vesicle pool. Nevertheless, flash-photolysis of caged calcium showed little difference in intrinsic calcium sensitivity of release when compared to control calyces. Based on this phenotype it was concluded that a perturbation of VAMP/synaptobrevin loosens the tight coupling between Ca^{2+} influx and vesicle release. Since this phenotype of VAMP/synaptobrevin perturbations is identical to the

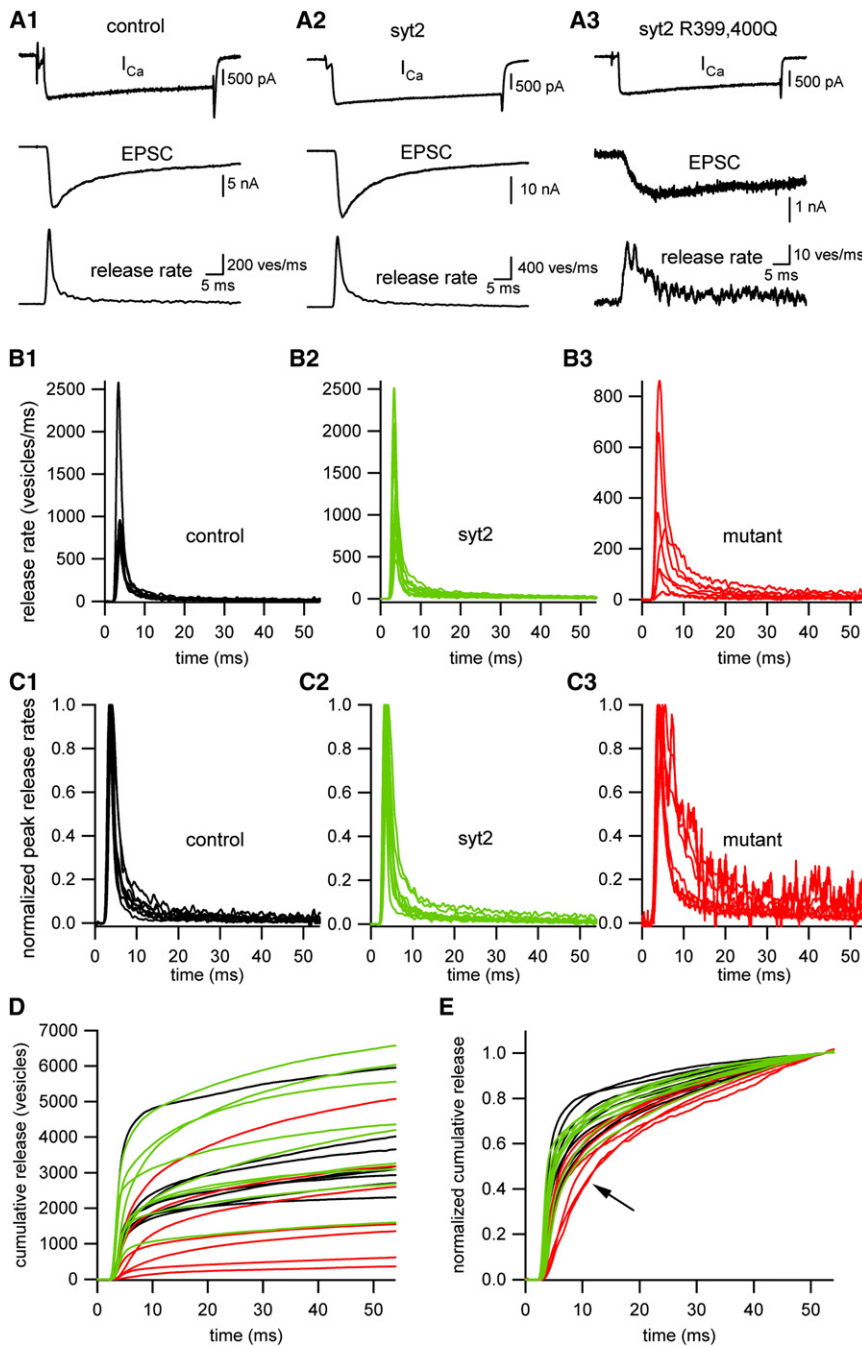


Figure 6. Deconvolution Analysis of Depleting Pulses Reveals that *syt2* R399,400Q Causes a Decrease in the Peak Release Rate and a Slowing of the Release of the Fast Pool

(A) Representative traces of control (A1), *syt2* (A2), or *syt2* R399,400Q (A3) calyces were identified and the presynaptic and postsynaptic compartments were voltage clamped to -80 mV. Traces shown from top to bottom are presynaptic calcium current, EPSC, and deconvolved release rate.

(B) Analyzed traces of release rates of control (B1), *syt2* (B2), or *syt2* R399,400Q (B3). ($n = 8$ control, $n = 9$ *syt2*, $n = 7$ *syt2* R399,400.)

(C) Analyzed traces of normalized peak release rates of control (C1), *syt2* (C2), or *syt2* R399,400Q (C3). ($n = 8$ control, $n = 9$ *syt2*, $n = 7$ *syt2* R399,400.)

(D) Integrated deconvolved release rates during the depleting pulse (cumulative release). (Control, black traces, $n = 8$; *syt2*, green traces, $n = 9$; *syt2*, R399,400Q, red traces, $n = 7$.)

(E) Normalized cumulative release. Traces in (D) were normalized with respect to the cumulative release at the end of the depleting pulse. The arrow indicates the slowing of the fast component of release in the *syt2* R399,400Q-positive calyces.

phenotype of R399,400Q mutation, we likewise conclude that intact *syt* is necessary for positional priming.

Recent reports characterizing this region of *syt* using liposomal fusion assays have reported contradictory results and suggested competing mechanisms (Arac et al., 2006; Gaffaney et al., 2008; Xue et al., 2008). One group has reported that this mutation interferes with *syt*'s ability to bind lipids in the plasma membrane, thus leading to a fusion defect (Arac et al., 2006; Xue et al., 2008), while another group has reported that this mutation interferes with *syt*'s ability to bind SNARE complexes (Gaffaney et al., 2008). Given

some controversies surrounding liposomal fusion assays and their relevance to synaptic physiology (Holt et al., 2008; Stein et al., 2007), it is difficult to judge the merits of the proposed models. Our results are well compatible with the model of Gaffaney et al. viewing *syt* as a mediator of the interaction between SNARE complexes and special sites at active zones. We do not see a way in which we can interpret our results in the context of the scheme proposed by Arac et al. (2006) and Xue et al. (2008). Previous reports have demonstrated the role of the SNARE complex in vesicle docking (de Wit et al., 2006; Stanley et al., 2003) and in the positioning of vesicles close to the release site (Sakaba et al., 2005; Stanley et al., 2003). If the R399,400Q mutation in *syt2* blocked the interaction of *syt* with SNAREs (Gaffaney et al., 2008), these

Mechanisms for the Reduction of the RRP by the *syt2* R399,400Q Mutation

The reduction of the RRP, which we observed in calyces strongly expressing *syt2* R399,400Q (Figures 5 and 6), may indicate that this region and *syt* in general have a role in vesicle priming or in stabilizing the primed pool. Defects in vesicle priming have been

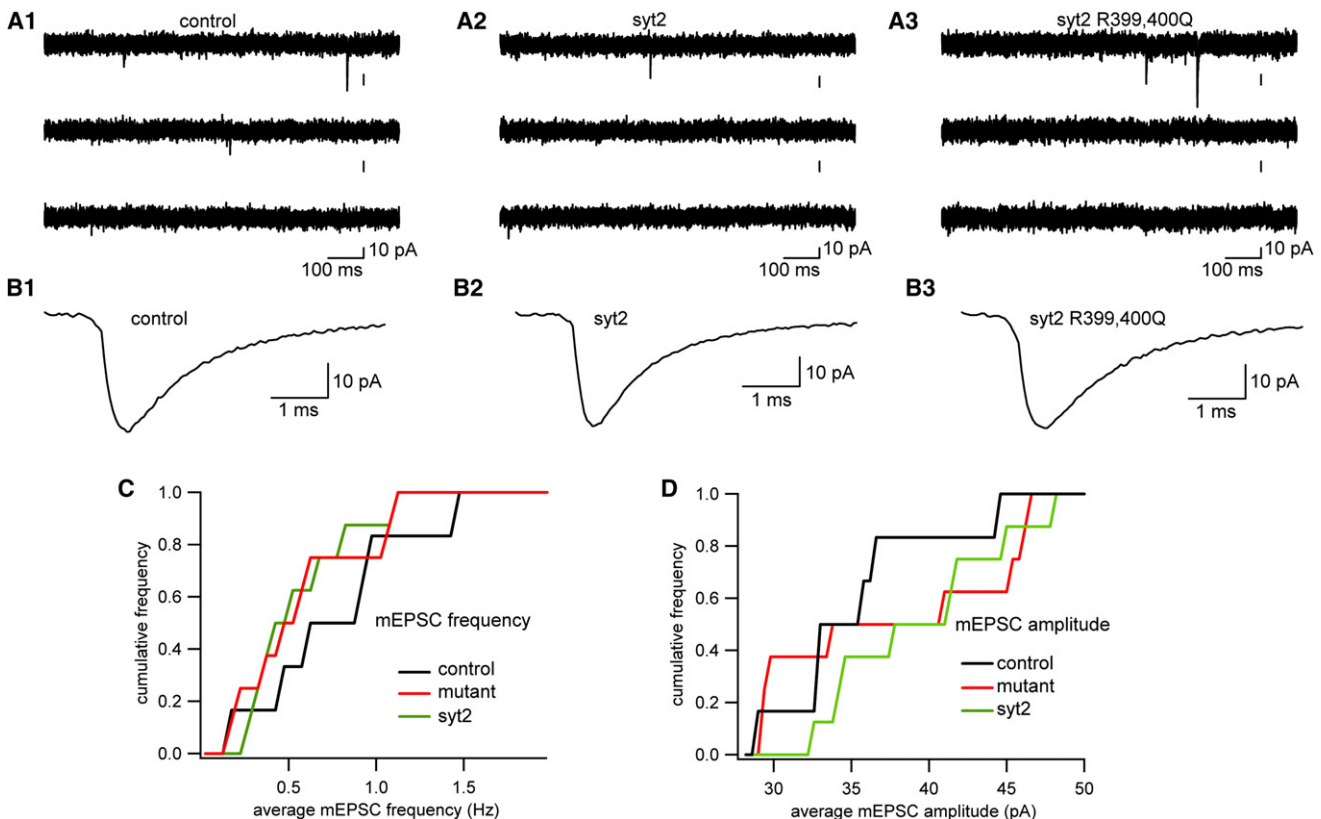


Figure 7. Overexpression of syt2 R399,400Q Does Not Cause a Change in mEPSC Frequency

(A) Representative traces of 3 continuous seconds of mEPSC recordings from P8 to P9 rats from principal neurons of the MNTB contacting control calyces (A1), syt2-overexpressing calyces (A2), or syt2 R399,400Q-overexpressing calyces (A3).

(B) Average miniwaveform from principal MNTB cells contacting control calyces (B1), syt2-overexpressing calyces (B2), or syt2 R399,400Q-overexpressing calyces (B3).

(C) Cumulative frequency histograms of average minifrequency values from syt2, syt2 R399,400Q, and control animals. Control (black traces), syt2 (green traces), and syt2 R399,400Q (red traces) are shown. (n = 6 control, n = 8 syt2, n = 8 syt2 R399,400Q.)

(D) Cumulative frequency histograms of average miniamplitude values from syt2, syt2 R399,400Q, and control animals. Control (black traces), syt2 (green traces), and syt2 R399,400Q (red traces) are shown.

shown to lead to a loss in the RRP (Brose et al., 2000). However, the effect of the syt2 R399,400Q mutation is more subtle. Xue et al. (2008) reported that the sucrose-sensitive RRP was unchanged between wild-type autaptic neurons and those expressing the reciprocal mutation in syt1 (R398,399Q), while Ca^{2+} -triggered release was strongly suppressed. To reconcile these findings with the results presented here, we have to assume that there is a pool of primed vesicles that is insensitive to Ca^{2+} , no matter whether $[\text{Ca}^{2+}]_i$ is increased via channel-mediated Ca^{2+} influx or uniformly via calcium uncaging (this work), but nevertheless is released by high osmolarity via sucrose application (Xue et al., 2008).

Unfortunately, the mechanism of sucrose action is not well understood and the validity of sucrose application as a measurement of the RRP is debated, because it has been reported to significantly overestimate the RRP size (Moulder and Mennerick, 2005; but see Stevens and Williams, 2007). We did not use sucrose application at the calyx because it does not allow accurate RRP determinations. Since sucrose responses are slow, complete pool depletion cannot be achieved, given the rapid

rates of pool refilling measured at this synapse (Hosoi et al., 2007). However, if vesicles were releasable in the calyx by sucrose, we would postulate that there are vesicles that, after strong overexpression of the R399,400Q mutant, have no functioning Ca^{2+} sensor and an otherwise normal release apparatus. Thus, these mutant molecules would still be part of the release machinery, although they would be unable to transmit their Ca^{2+} binding status to their interactors, even though it has been shown that Ca^{2+} binding is intact (Figure 7; Xue et al., 2008). This inability to transmit their Ca^{2+} binding status would lead to a failure to overcome the energy threshold for vesicle release, leading to a smaller RRP, while hyperosmotic sucrose application would lower the energy barrier for vesicle release, so that syt's ability to transmit its Ca^{2+} binding status to its interactors would no longer be needed.

Perturbations of syt and other interactors of the SNARE complex such as complexin (Brose, 2008) and snapin (Pan et al., 2009) have resulted in a wide variety of differential effects on synchronous versus asynchronous versus spontaneous release. In particular, deletion of predominant syt isoforms has

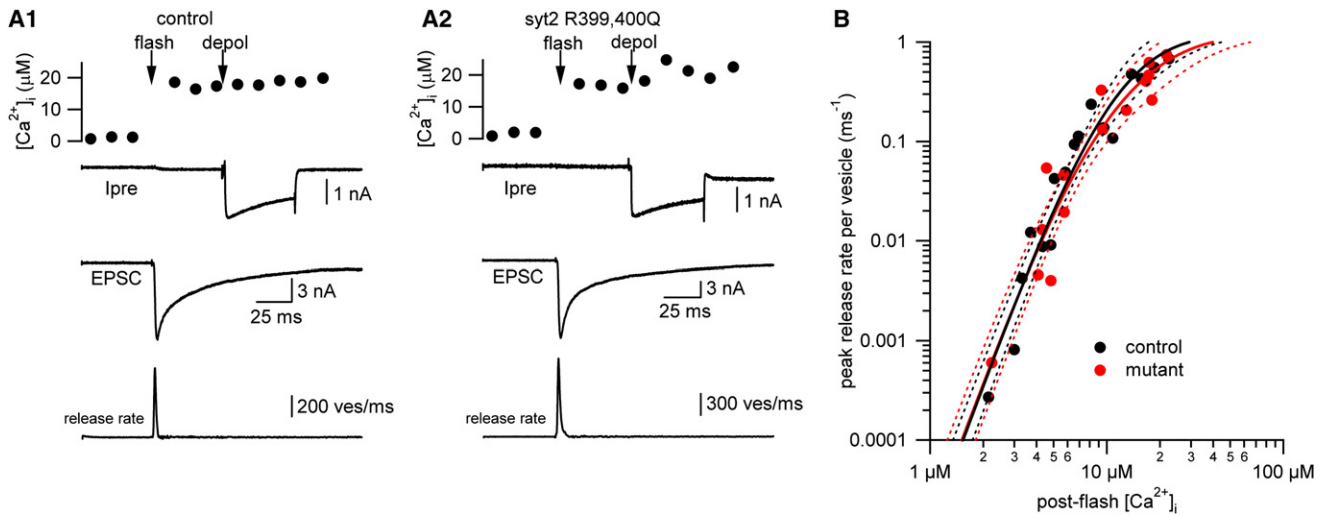


Figure 8. Syt2 R399,400Q Does Not Alter the Intracellular Calcium Sensitivity of Release

Flash-photolysis of caged calcium was performed using the calcium cage DM-nitrophen and $[Ca^{2+}]_i$ was measured using the ratiometric $[Ca^{2+}]_i$ indicator dye fura-2FF. A UV flash was given followed by a 50 ms depolarization after a 50 ms latency period. Prior to the flash, the pool size was estimated using a 50 ms depolarizing pulse as described in Figure 6. Sufficient time was given for recovery before flash-photolysis was performed. The peak release rate during the flash was then divided by the pool size estimate to determine the peak release rate per vesicle. (A) From top to bottom: presynaptic $[Ca^{2+}]_i$, Ca^{2+} -current, EPSC, and release rate. (A1), control; (A2), syt2 R399,400Q. (B) Peak release rate per vesicle versus post-flash $[Ca^{2+}]_i$. Control values are shown as black dots, while R399,400Q values are shown as red dots. $n = 9$ mutant pairs, $n = 8$ control pairs. Dotted lines represent 95% confidence intervals. Peak release rates per vesicle were fitted by a five-site release model with fusion rate γ and cooperativity factor b fixed to 6 ms^{-1} and 0.25, respectively. K_D values (k_{off}/k_{on}) for the mutant were $116.3\ \mu\text{M}$, and for the control, $137.4\ \mu\text{M}$.

led to increased spontaneous release in many preparations (Littleton et al., 1993; Pang et al., 2006b; Sun et al., 2007). Differential effects have usually been interpreted in terms of different properties of the release machineries for spontaneous and evoked release. So far, only in two cases have such differential effects been substantiated by an experimental demonstration of a change in the Ca^{2+} dose-response curve (Lou et al., 2005; Sun et al., 2007). We present here the first example of a molecular perturbation (apart from interference with clostridial toxins) that leads to differential effects on synchronous versus delayed release, as well as profound changes in short-term plasticity without a change in the intrinsic Ca^{2+} sensitivity of the release apparatus and without a change in the frequency of mEPSCs. Instead, we postulate that the mutation has an effect on the coupling between Ca^{2+} influx and the Ca^{2+} sensors for Ca^{2+} -triggered synchronous release.

Rapid neurotransmitter release in synchrony with APs requires an exquisite ultrastructural organization that allows interactions between ion channels and release ready vesicles at the shortest possible distances. It can be anticipated that a variety of molecular perturbations compromise this delicate assembly without affecting the core of the release machinery. The ability to quantitatively analyze synaptic transmission at the calyx of Held, in conjunction with the new ability to molecularly perturb this nerve terminal using viral vectors, allowed us to differentiate between functional steps in synaptic transmission and to uncover a second function of syt in synaptic transmission. Our new genetic tools will now allow for a dissection of multiple steps and a more complete understanding of the molecular mechanisms of synaptic transmission at mammalian synapses.

EXPERIMENTAL PROCEDURES

Animal Surgery

P1 Wistar rats were anesthetized with 95% O_2 mixed with 5% isoflurane using the CombiVet base system (Rothacher Medical, Bern, Switzerland) for 5 min. Afterwards, 50 μl of lidocaine solution was injected under the scalp and animals were placed into a Kopf stereotactic frame (Model 940 digital) (David Kopf Instruments, Tujunga, CA). A gas mask (Kopf) was placed over the animals' faces and animals were maintained under light anesthesia (0.6% to 0.8% isoflurane) using the CombiVet base system with humidifier (Rothacher). Animals were maintained at 37°C using an electronic thermometer linked to a heating pad (Harvard Apparatus, Holliston, MA). Using a scalpel, the scalp of the animal was opened and lambda relative to bregma was measured using a 32G blunt needle (Popper and Sons, Inc., New Hyde Park, NY). Typical coordinates for injection were (in mm, lambda relative to bregma) 0.200, A/P 4.9, L/R 1.7, D/V 6.2. A total of 3 μl rAd syt2 R399,400Q (2 μl of a 1.2×10^{12} particle/ml or rAd syt2 1.0×10^{12} particle/ml stock mixed with 1 μl of 20% mannitol in storage solution) was injected using a 32G blunt needle for 30 min at a rate of 100 nl/min. Subsequently, the needle was allowed to remain in place for 5 min, then slowly removed. Afterwards, the scalp was glued using Histoacryl (B. Braun Melsungen AG, Melsungen, Germany) and all traces of blood were removed. Anesthesia was stopped; animals were removed from the stereotactic frame and placed on a 37°C warm plate (Labotect GmbH, Goettingen, Germany). After full recovery, animals were placed back in their respective cages. Animals were sacrificed 7–8 days later. This procedure and all surgery experiments were carried out under the strict guidelines of the laws of Lower Saxony.

Creation of syt2 R399,400Q

Rat syt2 cDNA was codon optimized for expression in rat (Geneart, Regensburg, Germany). The codon-optimized syt2 was mutated at amino acid numbers 399,400 from arginine to glutamine using the primers 5'-GACATGCTGGCCAAACCCAGCAGCCATCGCCAGTGGCAC-3' and 5'-GTGCCACTGGCGATGGGCTGCTGGGGTTGGCCAGCATGTC-3'.

Mutagenesis was performed using the Quickchange strategy (Stratagene, La Jolla, CA). The mutations were then sequenced for verification. After creation of syt2 R399,400Q, it and the syt2 cDNA was cloned into the pUNISHER cassette described below.

Creation of pUNISHER

To ensure high levels of expression of syt2 R399,400Q, an expression cassette was made and cloned into the pDC511 plasmid (Microbix, Toronto, Canada). We call this the pUNISHER plasmid. pUNISHER combines previous optimizations of the transcriptional (Hioki et al., 2007), translational (Brun et al., 2003), and posttranscriptional signals (Brun et al., 2003; Wu et al., 2008; Xu et al., 2002) for transgene expression into one vector.

Construction of Virus

Second-generation Adenoviruses (Ad) containing the E2a deletion (Zhou and Beaudet, 2000) with slight modifications were made. The E2a deletion (Zhou et al., 1996) was cloned into the Fip,frt helper plasmid (Microbix). The 470 bp synapsin promoter (Kugler et al., 2001) driving EGFP expression was cloned into the E2a deletion region, so that the rAd syt2 R399,400Q virus expressed neurospecific EGFP independent of syt2 R399,400Q. The genomic helper plasmid and the pUNISHER plasmid were cotransfected into E2T cells following the standard protocols for rAd production (Ng and Graham, 2002). rAd was stored in 10 mM HEPES, 250 mM sucrose, and 1 mM MgCl₂ at pH 7.4.

To check for syt2 R399,400Q expression, primary hippocampal cultures were infected at 17 DIV and neurons were harvested 5 days postinfection. Approximately 60,000 neurons were loaded onto a 10% SDS PAGE gel and processed for western blot analysis using a syt2 polyclonal antibody (Synaptic Systems #105 023, Goettingen, Germany).

Slice Preparation

Acute brainstem slices were made from P8–P9 rats that had been injected with rAd syt2 R399,400Q or rAd syt2 at P1 or from age-matched control animals not transduced with virus, as previously described (Borst and Sakmann, 1996; Forsythe and Barnes-Davies, 1993). Using a Leica VTS 1000 vibratome (Leica, Wetzlar, Germany), 200 μ m slices of the brainstem including the MNTB were made in ice-cold solution containing, in mM, 125 NaCl, 2.5 KCl, 3 MgCl₂, 0.1 CaCl₂, 25 glucose, 25 NaHCO₃, 1.25 Na₂PO₄, 0.4 L-ascorbic acid, 3 myo-inositol, and 2 Na-pyruvate (pH 7.3–pH 7.4) at \sim 310 mOsm. Slices were immediately transferred to a chamber containing a similar solution at 36°C in which the CaCl₂ and MgCl₂ concentrations were changed to 2 mM and 1 mM, respectively. All solutions were bubbled continuously with 95% O₂ and 5% CO₂. Slices were allowed to recover for 1 hr and were then transferred to a recording chamber with the same solution at room temperature. For recordings the extracellular solution was supplemented with 1 μ M TTX (Alomone Labs, Jerusalem, IL), 10 mM TEA (Sigma, Steinheim, DE), 50 μ M DAP-5 (Tocris Biosciences, Bristol, UK), 100 μ M CTZ (Tocris), and 1 mM kynurenic acid (Kyn) (Tocris) as previously described (Sakaba and Neher, 2001b; Sakaba et al., 2002). Addition of DAP-5 leads to pharmacological isolation of AMPAR-mediated current. For flash-photolysis experiments 1 mM or 2 mM γ -DGG (Tocris) was substituted for Kyn, since Kyn absorbs UV light (Lou et al., 2005; Wadel et al., 2007).

Electrophysiology

For identification of cell pairs, slices were imaged using a CCD camera (Till Imago VGA, TILL Photonics, Graefelfing, Germany) through a 60x water immersion objective (Olympus 60x / 0.90W LUMPlanFl) on an upright Zeiss microscope (Axioskop) (Zeiss, Jena, Germany). To identify calyces transduced with the rAd syt2 R399,400Q virus, the slice was illuminated at an excitation wavelength of 480 nm using a Polychrome II Xenon bulb monochromator (TILL Photonics). The presynaptic and postsynaptic compartments of the calyx of Held/MNTB synapse were simultaneously voltage clamped to -80 mV using a HEKA EPC 9/2 amplifier controlled by the Pulse or Patchmaster software (HEKA, Lambrecht, DE). Recordings were low-pass filtered (6 kHz) and sampled at 50 kHz. Borosilicate patch pipettes (Hilgenberg Malsfeld, Germany) were pulled on a HEKA PIP-5 (HEKA). The presynaptic series resistance (R_s) was typically between 8–20 M Ω , and compensated electronically so that the residual R_s was 8 M Ω . For initial experiments presynaptic pipettes con-

tained, in mM, 140 Cs-gluconate, 10 HEPES, 20 TEA-Cl, 5 Na₂phosphocreatine, 4 Mg-ATP, 0.3 Na₂GTP, and 0.5 CsEGTA (final pH 7.3, \sim 340 mOsm). For flash experiments the presynaptic pipette contained, in mM, 130 Cs-gluconate, 20 HEPES, 5 Na₂ATP, 0.3 Na₂GTP, 0.5 MgCl₂, 20 TEA-Cl, 0.2 fura-2FF (Teflabs, Austin, TX), 2 DM-nitrophen (Calbiochem, LaJolla, CA), and 1.7 CaCl₂, with a final pH of 7.3 and an osmolarity of \sim 340 mOsm. The postsynaptic patch pipette contained, in mM, 140 Cs-gluconate, 10 HEPES, 20 TEA-Cl, 5 Na₂phosphocreatine, 4 Mg-ATP, 0.3 Na₂GTP, and 5 CsEGTA with a final pH of 7.3 and an osmolarity of \sim 320 mOsm. In addition, the extracellular solution for mEPSC omitted CTZ and Kyn, and included 5 μ M strychnine (Tocris) and 40 μ M bicuculline (Tocris) to block inhibitory inputs. Postsynaptic R_s was between 4–10 M Ω and compensated electronically so that only 3 M Ω remained. For mEPSC recordings only the principal neurons of the MNTB that contacted EGFP-positive calyces were patched and the postsynaptic R_s was not compensated electronically.

For Ca²⁺ uncaging, a UV flashlamp (Rapp Optoelectronic, Hamburg, Germany) with a photolysis duration of 1 ms was used to photolyze DM-nitrophen in the presynaptic terminal as previously described (Bollmann et al., 2000; Schneggenburger and Neher, 2000). The intracellular calcium concentration, [Ca²⁺]_i, was monitored by using the ratiometric Ca²⁺ dye fura-2FF (Teflabs), excited at 350 nm and 380 nm using a monochromator (Polychrome II, TILL Photonics). Time series images were analyzed offline using the TILLvisION software as previously described (Schneggenburger, 2005; Schneggenburger and Neher, 2000). [Ca²⁺]_i was calculated based on the calibration constants from in vitro measurements (R_{max} , R_{min} , and R_{int}) as previously described (Schneggenburger, 2005). All experiments were carried out at room temperature.

Analysis

IGOR PRO software (Wavemetrics, Portland, OR) was used for all offline data analysis. The residual R_s was compensated offline (Neher and Sakaba, 2001a). Data based on depolarizations (AP-like: -80 mV to $+40$ mV, 1 ms square wave pulses; long depolarizations: -80 mV to $+70$ mV for 2 ms, followed by 50 ms at 0 mV and then back to -80 mV) were plotted as cumulative frequency histograms. The peak amplitudes of the EPSCs were measured as peak minus baseline. Presynaptic calcium currents were converted to charge integrals. In the case of AP-like stimulation, the Ca²⁺ charge integral was calculated from the onset of the current to the point where 10% of the peak Ca²⁺ current remained. In the case of long depolarizations, the presynaptic calcium current was integrated from its onset (voltage step back to 0 mV) for the whole duration of the pulse (50 ms). Synaptic delays in response to AP-like stimulation were defined as the time at which the EPSC was 50% of its maximum minus the time of the peak of the calcium current. Synaptic delays in response to long depolarization were defined as the time at which EPSC was 50% of its maximum minus the time of the onset of the calcium current (the time when the depolarizing pulse was stepped back to 0 mV). For reporting of the EPSC amplitudes during paired pulse stimulation or 100 Hz stimulation, EPSC amplitudes were measured as differences between each peak value and its respective baseline and were then normalized to the first EPSC amplitude of the respective train. PPRs are reported as EPSC2/EPSC1. Similarly, PPR values of the calcium charge integral are reported as Ca²⁺ charge integral 2/Ca²⁺ charge integral 1.

For the analysis of synaptic delays in response to flash, traces were low-pass filtered offline using a Gauss filter (2 kHz cutoff). Synaptic delay was defined as the time when the EPSC crossed an absolute threshold of -100 pA minus the time point at which the flash lamp was triggered. Synaptic delay times were then plotted against [Ca²⁺]_i and binned into five different groups of [Ca²⁺]_i (four 5 μ M bins starting at 5 μ M and one bin from 3 μ M to 5 μ M). Means for each bin were calculated and a ratio of the mean delays (mutant/control) was calculated. Individual bin mean ratios were then averaged and reported as a grand mean \pm SEM.

For the analysis of mEPSCs, we used a custom-written mEPSC detection routine (Dr. Holger Taschenberger) based on Clements and Bekkers (1997). For inclusion of each cell in the data set, a minimum acquisition time of 60 s and a minimum of 15 recorded events were required. mEPSC frequency and mEPSC amplitude from each cell was averaged. Subsequently, the average

mEPSC frequency and mEPSC amplitude from each cell was used for statistical analysis comparing mEPSCs from control, *syt2*, and *syt2* R399,400Q calyces.

Statistics were carried using Prism (GraphPad, LaJolla, CA). A one-way ANOVA test was used if the data passed Bartlett's test of equal variance; if not, a Kruskal-Wallis test was used. In the case of the one-way ANOVA analysis, a post hoc Tukey test was used to compare all three groups to one another. In the case of the Kruskal-Wallis test, a post hoc Dunn's test was used to compare all three groups to one another.

Deconvolution Analysis

Deconvolution of the ESPCs from the long depolarization experiments and those from the flash-photolysis protocol were carried out as previously described (Lou et al., 2005; Neher and Sakaba, 2001a, 2003; Wadel et al., 2007). EPSCs were deconvolved with a double exponential mEPSC waveform (Scheuss et al., 2007), also taking into account the residual glutamate spillover current. Parameters for the time constants of mEPSCs and residual currents were empirically determined using the stimulus protocol as described by Neher and Sakaba (2001b). To determine if maximal flashes completely depleted the RRP, a long depolarizing pulse was applied 50 ms after flash onset (Wadel et al., 2007). To determine if there was a difference between the RRP as measured by the stand-alone 50 ms depolarization and the flash plus long depolarization, the RRP size of the 50 ms depolarization was divided by the RRP size measured by the flash plus long depolarization and reported as a ratio. The total RRP size was used to convert release rates into release rates per vesicle. These normalized rates were plotted against $[Ca^{2+}]_i$ on a log-log plot. Since there was variable penetrance of the *syt2* R399,400Q phenotype, criteria for inclusion of the data set for the mutant phenotype were established so that the EGFP-positive calyces with control-like phenotypes were eliminated. These criteria were that AP-like EPSC responses (1) must be less than 1 nA and (2) must be facilitated for a minimum of five pulses during a 20 AP 100 Hz train.

Release Model

The relationship between $[Ca^{2+}]_i$ and release rates per vesicles was modeled using a five-site kinetic model as originally described by Schneggenburger and Neher (2000) with slight modifications as described by Wang et al. (2008). To test the hypothesis that K_{10} values derived from the flash data differed significantly between the control and mutant, we performed a random permutation test (Wang et al., 2008) using 2000 samples. K_{10} values are reported as mean \pm bootstrap estimate of SEM. To test the hypothesis that there was no difference between the control and mutant model fits from the flash data, we formed ratios between peak release rates of mutant flash responses with respect to the control fit at the respective $[Ca^{2+}]_i$. Using Prism (GraphPad) software, mean and SEM of the logarithms of these ratios were calculated and a t test comparing the two groups or a one-sample t test was performed against hypothetical means of $\log_{10}1$ and $\log_{10}1/1.63$. We calculated mean and SEM of the logarithms of these ratios and obtained -0.0762 ± 0.07545 ($n = 15$). In addition, we also performed a t test comparing the log-ratio values from control (-0.008235 ± 0.05914 ; $n = 17$) to test the hypothesis that the two groups were different from each other. Gaussian distribution of log-ratio values was tested via a D'Agostino and Pearson omnibus normality test.

SUPPLEMENTAL DATA

Supplemental data for this article include one figure and can be found at [http://www.cell.com/neuron/supplemental/S0896-6273\(09\)00583-2](http://www.cell.com/neuron/supplemental/S0896-6273(09)00583-2).

ACKNOWLEDGMENTS

We thank Dr. Holger Taschenberger for help with the fitting of the flash data, IGOR programming, and minianalysis software. We thank Dr. Reinhard Jahn, Dr. Lu-Yang Wang, and Dr. Kristian Wadel for critical reading and comments on this manuscript; Dr. Christian Rosenmund for sharing unpublished *syt1* R398,399Q data; Dr. Kristian Wadel for suggesting the name "pUNISHER" for the new rAd vectors; and Dr. Irith Ginzburg for the gift of the tau 3' UTR. We thank the calyx group in the Department of Membrane

Biophysics for advice and support with the electrophysiology and Tanja Wiles for technical assistance. This work was supported by the Alexander von Humboldt Foundation, the Max Planck Society, and the European Commission (EU Synapse grant LSHM-CT-2005-019055).

Accepted: July 22, 2009

Published: August 26, 2009

REFERENCES

- Adler, E.M., Augustine, G.J., Duffy, S.N., and Charlton, M.P. (1991). Alien intracellular calcium chelators attenuate neurotransmitter release at the squid giant synapse. *J. Neurosci.* *11*, 1496–1507.
- Arac, D., Chen, X., Khant, H.A., Ubach, J., Ludtke, S.J., Kikkawa, M., Johnson, A.E., Chiu, W., Sudhof, T.C., and Rizo, J. (2006). Close membrane-membrane proximity induced by $Ca(2+)$ -dependent multivalent binding of synaptotagmin-1 to phospholipids. *Nat. Struct. Mol. Biol.* *13*, 209–217.
- Bennett, M.K., Calakos, N., and Scheller, R.H. (1992). Syntaxin: a synaptic protein implicated in docking of synaptic vesicles at presynaptic active zones. *Science* *257*, 255–259.
- Bollmann, J.H., Sakmann, B., and Borst, J.G. (2000). Calcium sensitivity of glutamate release in a calyx-type terminal. *Science* *289*, 953–957.
- Borst, J.G., and Sakmann, B. (1996). Calcium influx and transmitter release in a fast CNS synapse. *Nature* *383*, 431–434.
- Borst, J.G., and Sakmann, B. (1998). Facilitation of presynaptic calcium currents in the rat brainstem. *J. Physiol.* *513*, 149–155.
- Brose, N. (2008). For better or for worse: complexins regulate SNARE function and vesicle fusion. *Traffic* *9*, 1403–1413.
- Brose, N., Rosenmund, C., and Rettig, J. (2000). Regulation of transmitter release by Unc-13 and its homologues. *Curr. Opin. Neurobiol.* *10*, 303–311.
- Brun, S., Faucon-Biguot, N., and Mallet, J. (2003). Optimization of transgene expression at the posttranscriptional level in neural cells: implications for gene therapy. *Mol. Ther.* *7*, 782–789.
- Chapman, E.R. (2008). How does synaptotagmin trigger neurotransmitter release? *Annu. Rev. Biochem.* *77*, 615–641.
- Clements, J.D., and Bekkers, J.M. (1997). Detection of spontaneous synaptic events with an optimally scaled template. *Biophys. J.* *73*, 220–229.
- Cuttle, M.F., Tsujimoto, T., Forsythe, I.D., and Takahashi, T. (1998). Facilitation of the presynaptic calcium current at an auditory synapse in rat brainstem. *J. Physiol.* *512*, 723–729.
- de Wit, H., Cornelisse, L.N., Toonen, R.F., and Verhage, M. (2006). Docking of secretory vesicles is syntaxin dependent. *PLoS ONE* *1*, e126.
- Fernandez-Chacon, R., Shin, O.H., Konigstorfer, A., Matos, M.F., Meyer, A.C., Garcia, J., Gerber, S.H., Rizo, J., Sudhof, T.C., and Rosenmund, C. (2002). Structure/function analysis of Ca^{2+} binding to the C2A domain of synaptotagmin 1. *J. Neurosci.* *22*, 8438–8446.
- Forsythe, I.D., and Barnes-Davies, M. (1993). The binaural auditory pathway: excitatory amino acid receptors mediate dual timecourse excitatory postsynaptic currents in the rat medial nucleus of the trapezoid body. *Proc. Biol. Sci.* *251*, 151–157.
- Fukuda, M., Moreira, J.E., Liu, V., Sugimori, M., Mikoshiba, K., and Llinas, R.R. (2000). Role of the conserved WHXL motif in the C terminus of synaptotagmin in synaptic vesicle docking. *Proc. Natl. Acad. Sci. USA* *97*, 14715–14719.
- Gaffaney, J.D., Dunning, F.M., Wang, Z., Hui, E., and Chapman, E.R. (2008). Synaptotagmin C2B domain regulates Ca^{2+} -triggered fusion in vitro: critical residues revealed by scanning alanine mutagenesis. *J. Biol. Chem.* *283*, 31763–31775.
- Geppert, M., Goda, Y., Hammer, R.E., Li, C., Rosahl, T.W., Stevens, C.F., and Sudhof, T.C. (1994). Synaptotagmin I: a major Ca^{2+} sensor for transmitter release at a central synapse. *Cell* *79*, 717–727.
- Hata, Y., Davletov, B., Petrenko, A.G., Jahn, R., and Sudhof, T.C. (1993). Interaction of synaptotagmin with the cytoplasmic domains of neuroligins. *Neuron* *10*, 307–315.

- Han, W., Rhee, J.S., Maximov, A., Lao, Y., Mashimo, T., Rosenmund, C., and Sudhof, T.C. (2004). N-glycosylation is essential for vesicular targeting of synaptotagmin 1. *Neuron* 41, 85–99.
- Hioki, H., Kameda, H., Nakamura, H., Okunomiya, T., Ohira, K., Nakamura, K., Kuroda, M., Furuta, T., and Kaneko, T. (2007). Efficient gene transduction of neurons by lentivirus with enhanced neuron-specific promoters. *Gene Ther.* 14, 872–882.
- Holt, M., Riedel, D., Stein, A., Schuette, C., and Jahn, R. (2008). Synaptic vesicles are constitutively active fusion machines that function independently of Ca²⁺. *Curr. Biol.* 18, 715–722.
- Hosoi, N., Sakaba, T., and Neher, E. (2007). Quantitative analysis of calcium-dependent vesicle recruitment and its functional role at the calyx of Held synapse. *J. Neurosci.* 27, 14286–14298.
- Jorgensen, E.M., Hartweg, E., Schuske, K., Nonet, M.L., Jin, Y., and Horvitz, H.R. (1995). Defective recycling of synaptic vesicles in synaptotagmin mutants of *Caenorhabditis elegans*. *Nature* 378, 196–199.
- Krasnov, P.A., and Enikolopov, G. (2000). Targeting of synaptotagmin to neurite terminals in neuronally differentiated PC12 cells. *J. Cell Sci.* 113, 1389–1404.
- Kugler, S., Meyn, L., Holzmüller, H., Gerhardt, E., Isenmann, S., Schulz, J.B., and Bahr, M. (2001). Neuron-specific expression of therapeutic proteins: evaluation of different cellular promoters in recombinant adenoviral vectors. *Mol. Cell. Neurosci.* 17, 78–96.
- Leveque, C., Hoshino, T., David, P., Shoji-Kasai, Y., Leys, K., Omori, A., Lang, B., el Far, O., Sato, K., Martin-Moutot, N., et al. (1992). The synaptic vesicle protein synaptotagmin associates with calcium channels and is a putative Lambert-Eaton myasthenic syndrome antigen. *Proc. Natl. Acad. Sci. USA* 89, 3625–3629.
- Littleton, J.T., Stern, M., Schulze, K., Perin, M., and Bellen, H.J. (1993). Mutational analysis of *Drosophila* synaptotagmin demonstrates its essential role in Ca(2+)-activated neurotransmitter release. *Cell* 74, 1125–1134.
- Llinas, R., Sugimori, M., and Silver, R.B. (1992). Microdomains of high calcium concentration in a presynaptic terminal. *Science* 256, 677–679.
- Lou, X., Scheuss, V., and Schneggenburger, R. (2005). Allosteric modulation of the presynaptic Ca²⁺ sensor for vesicle fusion. *Nature* 435, 497–501.
- Mochida, S., Sheng, Z.H., Baker, C., Kobayashi, H., and Catterall, W.A. (1996). Inhibition of neurotransmission by peptides containing the synaptic protein interaction site of N-type Ca²⁺ channels. *Neuron* 17, 781–788.
- Moulder, K.L., and Mennerick, S. (2005). Reluctant vesicles contribute to the total readily releasable pool in glutamatergic hippocampal neurons. *J. Neurosci.* 25, 3842–3850.
- Neher, E., and Penner, R. (1994). Mice sans synaptotagmin. *Nature* 372, 316–317.
- Neher, E., and Sakaba, T. (2001a). Combining deconvolution and noise analysis for the estimation of transmitter release rates at the calyx of Held. *J. Neurosci.* 21, 444–461.
- Neher, E., and Sakaba, T. (2001b). Estimating transmitter release rates from postsynaptic current fluctuations. *J. Neurosci.* 21, 9638–9654.
- Neher, E., and Sakaba, T. (2003). Combining deconvolution and fluctuation analysis to determine quantal parameters and release rates. *J. Neurosci. Methods* 130, 143–157.
- Neher, E., and Sakaba, T. (2008). Multiple roles of calcium ions in the regulation of neurotransmitter release. *Neuron* 59, 861–872.
- Ng, P., and Graham, F.L. (2002). Construction of first-generation adenoviral vectors. *Methods Mol. Med.* 69, 389–414.
- Pan, P.Y., Tian, J.H., and Sheng, Z.H. (2009). Snapin facilitates the synchronization of synaptic vesicle fusion. *Neuron* 61, 412–424.
- Pang, Z.P., Melicoff, E., Padgett, D., Liu, Y., Teich, A.F., Dickey, B.F., Lin, W., Adachi, R., and Sudhof, T.C. (2006a). Synaptotagmin-2 is essential for survival and contributes to Ca²⁺ triggering of neurotransmitter release in central and neuromuscular synapses. *J. Neurosci.* 26, 13493–13504.
- Pang, Z.P., Sun, J., Rizo, J., Maximov, A., and Sudhof, T.C. (2006b). Genetic analysis of synaptotagmin 2 in spontaneous and Ca²⁺-triggered neurotransmitter release. *EMBO J.* 25, 2039–2050.
- Reist, N.E., Buchanan, J., Li, J., DiAntonio, A., Buxton, E.M., and Schwarz, T.L. (1998). Morphologically docked synaptic vesicles are reduced in synaptotagmin mutants of *Drosophila*. *J. Neurosci.* 18, 7662–7673.
- Sakaba, T. (2006). Roles of the fast-releasing and the slowly releasing vesicles in synaptic transmission at the calyx of held. *J. Neurosci.* 26, 5863–5871.
- Sakaba, T., and Neher, E. (2001a). Calmodulin mediates rapid recruitment of fast-releasing synaptic vesicles at a calyx-type synapse. *Neuron* 32, 1119–1131.
- Sakaba, T., and Neher, E. (2001b). Quantitative relationship between transmitter release and calcium current at the calyx of held synapse. *J. Neurosci.* 21, 462–476.
- Sakaba, T., Schneggenburger, R., and Neher, E. (2002). Estimation of quantal parameters at the calyx of Held synapse. *Neurosci. Res.* 44, 343–356.
- Sakaba, T., Stein, A., Jahn, R., and Neher, E. (2005). Distinct kinetic changes in neurotransmitter release after SNARE protein cleavage. *Science* 309, 491–494.
- Scheuss, V., Taschenberger, H., and Neher, E. (2007). Kinetics of both synchronous and asynchronous quantal release during trains of action potential-evoked EPSCs at the rat calyx of Held. *J. Physiol.* 585, 361–381.
- Schneggenburger, R. (2005). Ca²⁺ uncaging in nerve terminals. In *Imaging in Neuroscience and Development*, A. Konnerth and R. Yuste, eds. (Woodbury, NY: CSHL Press), pp. 415–419.
- Schneggenburger, R., and Neher, E. (2000). Intracellular calcium dependence of transmitter release rates at a fast central synapse. *Nature* 406, 889–893.
- Schneggenburger, R., and Forsythe, I.D. (2006). The calyx of Held. *Cell Tissue Res.* 326, 311–337.
- Schneggenburger, R., Meyer, A.C., and Neher, E. (1999). Released fraction and total size of a pool of immediately available transmitter quanta at a calyx synapse. *Neuron* 23, 399–409.
- Stanley, E.F., Reese, T.S., and Wang, G.Z. (2003). Molecular scaffold reorganization at the transmitter release site with vesicle exocytosis or botulinum toxin C1. *Eur. J. Neurosci.* 18, 2403–2407.
- Stein, A., Radhakrishnan, A., Riedel, D., Fasshauer, D., and Jahn, R. (2007). Synaptotagmin activates membrane fusion through a Ca²⁺-dependent trans interaction with phospholipids. *Nat. Struct. Mol. Biol.* 14, 904–911.
- Stevens, C.F., and Sullivan, J.M. (2003). The synaptotagmin C2A domain is part of the calcium sensor controlling fast synaptic transmission. *Neuron* 39, 299–308.
- Stevens, C.F., and Williams, J.H. (2007). Discharge of the readily releasable pool with action potentials at hippocampal synapses. *J. Neurophysiol.* 98, 3221–3229.
- Sun, J., Pang, Z.P., Qin, D., Fahim, A.T., Adachi, R., and Sudhof, T.C. (2007). A dual-Ca²⁺-sensor model for neurotransmitter release in a central synapse. *Nature* 450, 676–682.
- Takamori, S., Holt, M., Stenius, K., Lemke, E.A., Grønborg, M., Riedel, D., Urlaub, H., Schenck, S., Brügger, B., Ringler, P., et al. (2006). Molecular anatomy of a trafficking organelle. *Cell* 127, 831–846.
- Verhage, M., and Sørensen, J.B. (2008). Vesicle docking in regulated exocytosis. *Traffic* 9, 1414–1424.
- Wadel, K., Neher, E., and Sakaba, T. (2007). The coupling between synaptic vesicles and Ca²⁺ channels determines fast neurotransmitter release. *Neuron* 53, 563–575.
- Wang, L.Y., Neher, E., and Taschenberger, H. (2008). Synaptic vesicles in mature calyx of Held synapses sense higher nanodomain calcium concentrations during action potential-evoked glutamate release. *J. Neurosci.* 28, 14450–14458.
- Wimmer, V.C., Nevian, T., and Künér, T. (2004). Targeted in vivo expression of proteins in the calyx of Held. *Pflügers Arch.* 449, 319–333.

- Wu, Z., Sun, J., Zhang, T., Yin, C., Yin, F., Van Dyke, T., Samulski, R.J., and Monahan, P.E. (2008). Optimization of self-complementary AAV vectors for liver-directed expression results in sustained correction of hemophilia B at low vector dose. *Mol. Ther.* *16*, 280–289.
- Xu, J., and Wu, L.G. (2005). The decrease in the presynaptic calcium current is a major cause of short-term depression at a calyx-type synapse. *Neuron* *46*, 633–645.
- Xu, Z.L., Mizuguchi, H., Ishii-Watabe, A., Uchida, E., Mayumi, T., and Hayakawa, T. (2002). Strength evaluation of transcriptional regulatory elements for transgene expression by adenovirus vector. *J. Control. Release* *81*, 155–163.
- Xu, J., Mashimo, T., and Sudhof, T.C. (2007). Synaptotagmin-1, -2, and -9: Ca²⁺ sensors for fast release that specify distinct presynaptic properties in subsets of neurons. *Neuron* *54*, 567–581.
- Xue, M., Ma, C., Craig, T.K., Rosenmund, C., and Rizo, J. (2008). The Janus-faced nature of the C(2)B domain is fundamental for synaptotagmin-1 function. *Nat. Struct. Mol. Biol.* *15*, 1160–1168.
- Yoshihara, M., and Littleton, J.T. (2002). Synaptotagmin I functions as a calcium sensor to synchronize neurotransmitter release. *Neuron* *36*, 897–908.
- Zhou, H., and Beaudet, A.L. (2000). A new vector system with inducible E2a cell line for production of higher titer and safer adenoviral vectors. *Virology* *275*, 348–357.
- Zhou, H., O'Neal, W., Morral, N., and Beaudet, A.L. (1996). Development of a complementing cell line and a system for construction of adenovirus vectors with E1 and E2a deleted. *J. Virol.* *70*, 7030–7038.